Magnetic Iron Oxide Nanoparticles for Biomedical Applications

Kaiyi Jiang, **Linlin Zhang**, **Gang Bao**

Department of Bioengineering, Rice University, Houston, TX 77030

Abstract

Owing to the quantum confinement at the nanoscale, magnetic iron oxide nanoparticles (MIONs) consisting of magnetite and maghemite nanocrystals have unique physical properties, enabling a wide range of biomedical applications by utilizing mechanical, magnetic, chemical, and thermal effects of MIONs respectively. For example, MIONs can serve as a contrast agent for magnetic resonance imaging (MRI), convert electromagnetic energy into thermal energy for hyperthermia therapy, and carry drug/gene for targeted *in vivo* delivery. In this review, we discuss the recent development of MION based engineering approaches and their biomedical applications, including sensitive protein quantification, magnetic nanoparticle heating, *in vivo* molecular imaging, and drug delivery. The opportunities and challenges in further exploring the biomedical applications of MIONs are also briefly discussed.

Keywords

magnetic iron oxide nanoparticles; magnetic heating; molecular imaging; protein detection

Introduction

Over the last few decades, nanotechnology including nanomaterials and nanodevices has emerged as an enabling and transformative technology that can be applied to disease detection and therapy [1–3]. Of all the nanomaterials developed, magnetic iron oxide nanoparticles (MIONs), magnetite (Fe_3O_4) or maghemite (γ-Fe_2O_3) having at least one dimension within 1 to 100 nm, have enjoyed a wide range of applications due to its low toxicity, high biocompatibility, and unique mechanical, magnetic, chemical, and thermal effects under different applied magnetic fields [1, 4–6]. For example, magnetic targeting with MIONs under an applied magnetic field has been used to remotely control the delivery of a variety of cargos such as small molecule drugs, therapeutic proteins and viral vectors to target specific tissue *in vivo* [7–11]. Many MIONs are being tested in clinical trials and several MION based systems have been approved by the Food and Drug Administration (FDA) for clinical applications [1, 12], including dextran coated MION contrast agent AMI-25 (Ferumoxide, Feridex IV, Endorem) for liver and spleen imaging [13].

Conflict of Interest Statement

The authors declare no conflict of interest.

The biomedical applications of MIONs are based on the functions of MIONs derived from their unique nanoscale physical properties under static or dynamic magnetic fields. For example, MIONs experience magnetic forces in a nonuniform magnetic field (Figure 1A), which can apply forces to cell surface proteins to actuate receptor-mediated signaling or to alter cell-cell interactions [14, 15]. The magnetic forces can also attract MIONs to certain locations or prevent them from moving out of the volume of interest. Iron oxide nanocryatals can generate T_1 or T_2 contrasts for MRI (Figure 1B) which, unlike the commonly used MRI contrast agent gadolinium, are non-toxic. Therefore, MIONs have been used as a contrast agent for MRI-based *in vivo* molecular imaging and cell tracking [5, 16, 17]. Under an alternating magnetic field, MIONs can generate a large amount of heat (magnetic heating) (Figure 1C), enabling hyperthermia therapy of cancer with locally elevated temperature [18, 19]. These three major types of MION functions, force generation, MRI contrast, and magnetic heating illustrate the unique capabilities of MIONs compared with other nanomaterials [1].

In this review, we discuss recent progress in developing MION based approaches for disease detection and therapy. We first briefly review the synthesis and coating of MIONs, then highlight the applications of MIONs in four areas: in vitro protein detection, magnetic heating, *in vivo* imaging, and *in vivo* drug delivery, utilizing the chemical, mechanical, thermal and imaging contrast properties of MIONs. The opportunities and challenges in further exploring the biomedical applications of MIONs are also discussed.

MION Properties, Synthesis and Coating

The magnetic properties of magnetite and maghemite nanocrystals are distinct from those of bulk materials owing to the unique quantum mechanical effects at the nanoscale. At the length scale less than the magnetic domain wall width (ca. 80–90 nm), these nanocrystals support only one magnetic domain, in which the spins of unpaired electrons are coupled to behave as a macro magnetic spin [20]. As the nanocrystal size further decreases below a superparamagnetic limit (ca. 20 nm), the thermal fluctuation becomes large enough to overcome the energy barrier arising from the magnetic anisotropy. The magnetic moment of individual nanocrystals flips rapidly among the easy axes, a process known as the Néelian relaxation, and no net magnetization can be observed. The magnetization of the nanocrystals will rapidly approach saturation magnetization when exposed to a modest magnetic field (0.2–0.5 Tesla). These nanocrystals are thus named superparamagnetic iron oxide nanoparticles (SPIOs). It has been shown that SPIOs can be used as T_1 or T_2 contract agents for MRI [21, 22].

In order for MIONs to have the desired functions in biomedical applications, the magnetic proprieties of MIONs as well as their size, size distribution and surface chemistry need to be optimized during synthesis of nanocrystals and the coating process [23]. Iron oxide nanocrystals with different morphology and surface chemistry can be generated by various methods including chemical, physical and biological methods [23]. While physical methods such as deposition of gas phase and electron beam lithography, and biological methods using magnetotactic bacteria enable reproducible production of MIONs [24–26], they often cannot produce MIONs with the desired size and/or surface chemistry. Thus, chemical-based

synthesis methods such as thermal decomposition and coprecipitation have been widely used due to high yield and controllability, and low production cost [1]. During coprecipitation synthesis, nanocrystals are generated by mixing ferrous and ferric salts stoichiometrically in an aqueous medium and precipitating ferrous and ferric ions with a base [27]. Polymers such as dextran and starch are often present in the reaction to generate a surface layer on the nanocrystals to render MIONs biocompatible and water-soluble. Although coprecipitation is simple, cost-efficient and scalable thus being used widely, it lacks good control over crystal growth, often resulting in polydisperse MIONs, and requiring post-synthesis size selection [28].

In contrast, thermo-decomposition method allows fine control of nanocrystal growth and the generation of monodisperse nanocrystals [29, 30]. This method decomposes a precursor compound such as iron oleate in organic solvents at high temperature to generate "Fe-O" monomer and form nanocrystal seeds. Thermo-decomposition separates the nucleation of seed and growth of seed to better control the size of nanocrystals. It has been shown that through fine tuning of reaction conditions such as concentration of precursor, capping agent and incubation temperature, one can generate highly uniform and monodisperse MIONs of various sizes (Figure 1D).

As synthesized MIONs with capping agents such as oleic acid often aggregate in water due to hydrophobic nature of the surface molecules, or magnetic attraction if the size of nanocrystal is larger than 20 nm. It is thus necessary to coat MIONs with hydrophilic molecules to render them stable and monodisperse in water and biological media [31–33], For most biomedical applications, the coating layer can also minimize immunogenicity and provide a means for functionalization [1]. Although dextran and starch are commonly used surface molecules for coating MIONs, polyethylene glycol (PEG) has gained much attention in recent years as PEG is minimally immunogenic and biocompatible, thus suitable for *in vivo* applications. A dual solvent exchange method was developed to achieve better control of surface density of PEG and the amount of reactive groups on MION surface, thus significantly improving the PEG coating efficiency and quality [34]. Other coating materials such as mesoporous silica, lipids and proteins have also been used to coat MIONs [35–37]. Coated MIONs can be functionalized with targeting antibodies or peptides, and carry fluorophores, siRNA and drug molecules for disease detection and therapy (Figure 1E) [38, 39].

In vitro protein detection

With the recent progress in proteomics, a large number of biomolecules including proteins have been identified as disease markers for the detection and diagnosis of cancer, autoimmune disease and infectious disease [40–42] However, most clinical quantification of protein concentration in human blood samples still rely on enzyme linked immunosorbent assay (ELISA), which can be effected by heat, radiation and oxidants [43]. In addition, the use of ELISA often requires well trained technicians to generate the standard curve for quantification. Thus, there is a need to develop point-of-care protein detection kits that are easy to use and insensitive to environmental changes. Although label-free detection

of proteins using gold nanoparticles has been developed [44], the use of aptamers or aggregation for detection and quantification limits its application.

MIONs can serve as a nanoparticle-based platform for rapid, sensitive and reliable protein detection. Figures 2A and 2B illustrate schematically the iron oxide nanoparticle linked immunosorbent assay (ILISA) as an example of MION based protein detection assays [43, 45]. Similar to a sandwich ELISA assay, in this work, Wüstite MIONs are functionalized with antibody fragment to act as the detection probe (Figure 2A). Target proteins are captured by the capture molecules (usually antibodies) on a surface and the detection probes bind to the target proteins, with unbound probes are removed by washing. The bound MION nanocrystals are dissolved by acid lysis and the amount of released iron atoms are quantified through a chromogenic reaction (Figure 2B)[45]. In the ILISA assay, that signal amplification is fully defined by the size and atom density of nanocrystals, which can be optimized through well-controlled nanocrystal synthesis. Signal amplification in ILISA is through stoichiometric chromogenesis of MIONs, which is insensitive to oxidants, radiation and heat, thus serves as a better signal readout than conventional enzymatic catalysis or direct amplification using fluorophore conjugated on antibodies.

It has been shown that ILISA has very high sensitivity in detecting proteins at very low (sub-picomolar) concentrations and exhibits a wide dynamic range [43, 45], and can be used in quantifying IgG and IgM antibodies in human serum samples from patients infected with respectively West Nile virus (WNV) and human herpes virus (HHV) (Figure 2C). With careful synthesis and functionalization of the MION probes, ILISA based protein detection assays can be performed using a universal standard curve, thus are simpler and more robust, having the potential to be used in point-of-care diagnostic applications.

Magnetic Heating

The ability to generate heat under an alternating magnetic field (AMF) is a very important property of MIONs (Figure 1C), which has been exploited in hyperthermia therapy of cancer [18, 19, 46, 47]. There have been extensive theoretical modeling and experimental studies on the magnetic heating mechanisms, as well as efforts to increase the heating capacity of MIONs through better synthesis [47–51]. Many theoretical models have been developed to better understand the magnetic heating properties of MIONs. In particular, the linear response theory (LRT) has been widely accepted and the LRT model predicts that MIONs with ~14 nm diameter has the maximum heating capacity under an AMF of 300 kHz [52, 53], which was supported by some experiments [54, 55]. However, through an extensive study of single-domain magnetic iron oxide nanoparticles, it was found that, contrary to the LRT model, MIONs larger than 14 nm can achieve higher heating capacity [47]. For example, under AMF of 325 kHz and 20.7 kA/m field strength, the specific absorption rate (SAR) of 40 nm MIONs is 2560 W/g Fe, 50 times higher than that of 11 nm MIONs [47]. (Figure 3A). A modified dynamic hysteresis model was developed to better characterize the magnetic heating behaviors of MIONs [47]. Similarly, it was found that 45 nm MIONs reside in a graphene oxide sheet had a SAR value of 5,020 W/g Fe under an AFM of 400 kHz and 32.5 kA/m field strength [49] (Figure 3B), confirming that large MIONs have much higher heat capacity than the LRT model predicted.

MIONs have the potential for targeted hyperthermia treatment of cancer [18, 56]. It has been shown that, with 40 nm MIONs injected into a mouse tumor model, the temperature in tumor tissue increased to 43°C within one hour of magnetic heating, high enough to trigger tumor cell death (Figure 3C). However, the use of locally injected MIONs in hyperthermia treatment may suffer from low retention time of MIONs in the tumor. Recently, Zhang et al described a method in which hydrogel loaded with MIONs was used for multiple hyperthermia treatments with a single injection [18], demonstrating tumor temperature increase to ~43°C even at the 4th round of heating, allowing for efficient removal of tumor in mice (Figure 3D). With doped MIONs and better coatings, MIONs can generate the desired temperature increase *in vivo* with reduced dose and lower field frequency and strength [49, 54, 57].

In vivo imaging and drug delivery

Over the last two decades MIONs have been used as imaging contrast agents for MRI based disease detection and for targeted delivery of drug molecules [58]. MIONs generate MRI imaging contrast through changing the relaxation of surrounding water protons when they are excited by the radio frequency and subsequently return to equilibrium state. Many groups have shown that MIONs can be used as an MRI contrast agent for *in vivo* molecular imaging and tuning of T_1 and T_2 relaxation time can be achieved through changing the size, chemical composition of nanocrystals, and different surface ligands [22, 59, 60]. MIONs have been optimized for *in vivo* imaging by changing their shape or surface coating. For example, Wei *et al* has described a method in which superparamagnetic MIONs are coated with zwitterion to enable enhanced T_1 weighted contrast in MRI [61]. Zhao *et al* used MIONs as a T_2 weighted MRI contrast imaging by changing the shape of MIONs to octapod [62]. For biomedical applications, it is also important to determine tissue toxicity, biodistribution, and renal clearance of MIONs [60, 63, 64].

MIONs can also be functionalized with different fluorophores on the surface that enable florescence imaging (FI) [65, 66]. Recently, multimodality imaging that combines MRI and FI has been developed in which MIONs are used to perform both deep tissue *in vivo* imaging via MRI and fluorescence imaging with tissue sections [5, 67, 68]. In particular, it has been shown that near infrared fluorescence (NIRF) dyes like Cy5.5 can be conjugated to MIONs through thermal crosslinking using Si-OH containing co-polymer or dextran [69, 70] and this enables MIONs to be used for enhanced *in vivo* dual modality cancer imaging. In addition to MRI/FI dual modality imaging, MRI/CT imaging has also been explored with MIONs that are doped with gold, since gold nanoparticles are commonly used as an X-ray contrast agent [71, 72].

In addition to using MIONs for molecule imaging, MIONs can be used to deliver drugs/ genes and other cargo molecules *in vivo*, and to track the efficiency of cargo delivery to the target tissue, and determine the biodistribution [73]. With MIONs' high surface to volume ratio, MION based drug delivery systems have the potential to be used in a variety of disease therapies [46, 73, 74]. For example, MIONs coated with PEG-DOX-indocyanine green (ICG) are able to deliver Doxorubicin (DOX) into tumor, while ICG allows fluorescence imaging of the DOX-loaded MIONs [65]. As shown in Figure 4A,

at 24 hours, fluorescence imaging shows that the majority of drug molecules are retained in the brain tumor demonstrating the enhanced accumulation through the use of MIONs. Recently, magnetic particle imaging (MPI) has been utilized to monitor the release of drug molecules *in vivo* [75]. Using Fe_3O_4 nanoclusters that degrade under mild acidic environment, it was demonstrated that MPI signal changes linearly with the release of DOX from the nanoclusters (Figure 4B), and the MPI signals showed that DOX continues to accumulate in the tumor for up to 48 hours post injection. MPI imaging can accurately track the delivery of drug molecules to the target tissue, enabling quantitative monitoring of cargo delivery. MIONs can be functionalized with antibodies or peptides for targeted *in vivo* delivery, to increase the accumulation of drugs (including small molecule drugs and proteins) in the diseased tissue and reduce the 'off-target' tissue delivery that may cause side effects [1]. As an example of targeted delivery of drug molecules to tumor cells, EGFRvIII antibody conjugated MIONs have been used to target glioblastoma [76]. Kohler *et al* conjugated methotrexate (MTX), a chemotherapeutic agent targeting cancer cells, to MIONs and demonstrated intracellular uptake of the MIONs by tumor cells and subsequent drug release inside the cells [77]. Conjugating different peptides such as cell penetrating peptides or peptides that target over-expressed proteins on cancer cell surface have also been explored for enhanced delivery of MIONs to the target cells [78, 79].

MIONs based drug delivery system can effectively cross the blood brain barrier (BBB) that enables better delivery of drug molecules such as DOX, which often suffer poor permeability through the blood-brain barrier [65]. MIONs can also be used in magnetic targeting, i.e., using a magnetic field to remotely control the distribution of drug molecules in the body, thereby enhancing drug accumulation in the target tissue [80]. The vascular endothelium presents a major obstacle for most conventional drug delivery methods as blood vessels selectively extravasate solutes and molecules at limited rates. It has been demonstrated recently that magnetic targeting of MIONs can be used to disrupt the endothelial adherent junctions as internalized MIONs in the endothelial cells lining blood vessels generate molecular forces and increase the vascular permeability [15] (Figure 4C). As shown in Figure 4D, prior to the application of external magnetic field, actin filaments (red) are aligned with the flow and anti-VE-cadherin staining (green) shows continuous adherent junctions. After an external magnetic field is applied for 1 hour below the channel, we observed disrupted adherent junctions as shown by the actin filament fiber and cadherin staining. Through the generation of magnetic force from the MIONs internalized in the endothelial cells, the number of actin filaments along the flow direction was reduced and the distribution of VE-cadherin became discontinuous and diffuse, indicating the disruption of adherent junctions at intercellular interfaces. We found that this process is reversible after the magnetic field is removed, and the continuous adherens junctions can be restored overnight (~10 hours).

The use of MIONs can remotely alter the cytoskeletal organizations of endothelial cells and activate the paracellular transport pathway that facilitate the uptake of all circulating agents [15]. This method enables a generalizable platform to control the paracellular uptake of drugs through magnetic control and can be applied to increase the uptake of any injectable pharmaceutical products.

Concluding Remarks

As precision medicine gradually takes shape to replace the current "one size fits all" clinical strategy, the field of nanomedicine, including that using MION based systems, has unprecedented opportunities to generate a large clinical impact. The unique nanoscale features of MIONs such as force generation, magnetic heating and imaging contrast render them an ideal platform to engineer translatable tools for the next-generation precision medicine. However, challenges exist in order to further improve the MION systems for biomedical applications, including scale up of nanocrystal synthesis and low-cost, highly efficient coating processes. To improve the quality of MION nanocrystals, a better understanding of the chemical reaction during thermodecomposition should be established to fine-tune the synthesis of MIONs with the desired size and morphology, and a better coating method is needed to allow large (>25 nm) MIONs to remain stable without aggregation in biologically relevant media. For heat generation by MIONs under AMF, a more sophisticated model needs to be developed to predict SAR as function of MION size under a wide range of frequency ($10^2 - 10^9$ Hz) and field strength (0.1–100 kA/m). It is possible to increase anisotropy constant (thus SAR) through surface modifications and metal doping of MIONs.

Immunotherapy has emerged as a promising strategy against cancer, autoimmune diseases and other chronic diseases. A better understanding of how MIONs interact with immune cells *in vivo* is required in order to use MIONs to improve immunotherapies through modulation of the immune response. There are opportunities to synergistically utilize multiple properties of MIONs, such as combining imaging contrast, heat generation and the use of magnetic force to have targeted, image-guided and controlled delivery and release of drugs/genes *in vivo* for nanotherapies with high efficiency and safety. A coordinated effort in bioengineering, chemistry, and material science will enable the development of next-generation MIONs for precision medicine, and help translate the MION-based technologies into impactful clinical products.

Acknowledgements

Abbreviations

MION	magnetic iron oxide nanoparticles
MRI	magnetic resonance imaging
FI	florescence imaging
PEG	polyethylene glycol
ELISA	enzyme linked immunosorbent assay
ILISA	iron oxide nanoparticle linked immunosorbent assay
AMF	alternating magnetic field

LRT	linear response theory
ICG	indocyanine green
DOX	Doxorubicin
MPI	magnetic particle imaging

Reference

[1]. Tong S, Zhu H, Bao G, Magnetic iron oxide nanoparticles for disease detection and therapy, Materials Today 31 (2019) 86–99. [PubMed: 32831620] * This is a comprehensive review of the synthesis and functionalization of magnetic iron oxide nanoparticles for biomedical applications

[2]. Brede C, Labhasetwar V, Applications of Nanoparticles in the Detection and Treatment of Kidney Diseases, Advances in Chronic Kidney Disease 20(6) (2013) 454–465. [PubMed: 24206598]

[3]. Noukeu LC, Wolf J, Yuan B, Banerjee S, Nguyen KT, Nanoparticles for Detection and Treatment of Peripheral Arterial Disease, Small 14(32) (2018) 1800644.

[4]. Feng Q, Liu Y, Huang J, Chen K, Huang J, Xiao K, Uptake, distribution, clearance, and toxicity of iron oxide nanoparticles with different sizes and coatings, Scientific Reports 8(1) (2018) 2082. [PubMed: 29391477]

[5]. Zhang L, Tong S, Zhang Q, Bao G, Lipid-Encapsulated Fe3O4 Nanoparticles for Multimodal Magnetic Resonance/Fluorescence Imaging, ACS Applied Nano Materials 3(7) (2020) 6785–6797. * A recent demonstration of MIONs as a dual-modality imaging probe for combined MRI and fluorescence imaging

[6]. Santra S, Kaittanis C, Grimm J, Perez JM, Drug/Dye-Loaded, Multifunctional Iron Oxide Nanoparticles for Combined Targeted Cancer Therapy and Dual Optical/Magnetic Resonance Imaging, Small 5(16) (2009) 1862–1868. [PubMed: 19384879]

[7]. Widder KJ, Morris RM, Poore G, Howard DP, Senyei AE, Tumor remission in Yoshida sarcoma-bearing rts by selective targeting of magnetic albumin microspheres containing doxorubicin, Proceedings of the National Academy of Sciences 78(1) (1981) 579–581.

[8]. Landázuri N, Tong S, Suo J, Joseph G, Weiss D, Sutcliffe DJ, Giddens DP, Bao G, Taylor WR, Magnetic Targeting of Human Mesenchymal Stem Cells with Internalized Superparamagnetic Iron Oxide Nanoparticles, Small 9(23) (2013) 4017–4026. [PubMed: 23766267]

[9]. Etoc F, Vicario C, Lisse D, Siaugue J-M, Piehler J, Coppey M, Dahan M, Magnetogenetic Control of Protein Gradients Inside Living Cells with High Spatial and Temporal Resolution, Nano Letters 15(5) (2015) 3487–3494. [PubMed: 25895433]

[10]. Namiki Y, Namiki T, Yoshida H, Ishii Y, Tsubota A, Koido S, Nariai K, Mitsunaga M, Yanagisawa S, Kashiwagi H, Mabashi Y, Yumoto Y, Hoshina S, Fujise K, Tada N, A novel magnetic crystal–lipid nanostructure for magnetically guided in vivo gene delivery, Nature Nanotechnology 4(9) (2009) 598–606.

[11]. Hofmann A, Wenzel D, Becher UM, Freitag DF, Klein AM, Eberbeck D, Schulte M, Zimmermann K, Bergemann C, Gleich B, Roell W, Weyh T, Trahms L, Nickenig G, Fleischmann BK, Pfeifer A, Combined targeting of lentiviral vectors and positioning of transduced cells by magnetic nanoparticles, Proceedings of the National Academy of Sciences 106(1) (2009) 44–49.

[12]. Nardecchia S, Sánchez-Moreno P, Vicente JD, Marchal JA, Boulaiz H, Clinical Trials of Thermosensitive Nanomaterials: An Overview, Nanomaterials 9(2) (2019) 191.

[13]. Taylor PM, Hawnaur JM, Hutchinson CE, Superparamagnetic iron oxide imaging of focal liver disease, Clinical Radiology 50(4) (1995) 215–219. [PubMed: 7729116]

[14]. Mannix RJ, Kumar S, Cassiola F, Montoya-Zavala M, Feinstein E, Prentiss M, Ingber DE, Nanomagnetic actuation of receptor-mediated signal transduction, Nature Nanotechnology 3(1) (2008) 36–40.

[15]. Qiu Y, Tong S, Zhang L, Sakurai Y, Myers DR, Hong L, Lam WA, Bao G, Magnetic forces enable controlled drug delivery by disrupting endothelial cell-cell junctions, Nature Communications 8(1) (2017) 15594.

[16]. Jeon M, Halbert MV, Stephen ZR, Zhang M, Iron Oxide Nanoparticles as T(1) Contrast Agents for Magnetic Resonance Imaging: Fundamentals, Challenges, Applications, and Prospectives, Adv Mater (2020) e1906539. [PubMed: 32495404] * This is a recent review on iron oxide nanoparticles as T1 contrast agents for MRI, and it's potential to serve as an alternative to gadolinium-based chelates.

[17]. Lewin M, Carlesso N, Tung C-H, Tang X-W, Cory D, Scadden DT, Weissleder R, Tat peptide-derivatized magnetic nanoparticles allow in vivo tracking and recovery of progenitor cells, Nature Biotechnology 18(4) (2000) 410–414.

[18]. Zhang ZQ, Song SC, Thermosensitive/superparamagnetic iron oxide nanoparticle-loaded nanocapsule hydrogels for multiple cancer hyperthermia, Biomaterials 106 (2016) 13–23. [PubMed: 27543919]

[19]. Maier-Hauff K, Ulrich F, Nestler D, Niehoff H, Wust P, Thiesen B, Orawa H, Budach V, Jordan A, Efficacy and safety of intratumoral thermotherapy using magnetic iron-oxide nanoparticles combined with external beam radiotherapy on patients with recurrent glioblastoma multiforme, Journal of Neuro-Oncology 103(2) (2011) 317–324. [PubMed: 20845061]

[20]. Krishnan KM, Pakhomov AB, Bao Y, Blomqvist P, Chun Y, Gonzales M, Griffin K, Ji X, Roberts BK, Nanomagnetism and spin electronics: materials, microstructure and novel properties, J Mater Sci 41(3) (2006) 793–815.

[21]. Iqbal MZ, Ma X, Chen T, Zhang L, Ren W, Xiang L, Wu A, Silica-coated superparamagnetic iron oxide nanoparticles (SPIONPs): a new type contrast agent of T(1) magnetic resonance imaging (MRI), J Mater Chem B 3(26) (2015) 5172–5181. [PubMed: 32262592]

[22]. Tong S, Hou S, Zheng Z, Zhou J, Bao G, Coating Optimization of Superparamagnetic Iron Oxide Nanoparticles for High T2Relaxivity, Nano Letters 10(11) (2010) 4607–4613. [PubMed: 20939602]

[23]. Ali A, Zafar H, Zia M, Ul Haq I, Phull AR, Ali JS, Hussain A, Synthesis, characterization, applications, and challenges of iron oxide nanoparticles, Nanotechnology, Science and Applications 9 (2016) 49–67.

[24]. Genove G, Demarco U, Xu H, Goins WF, Ahrens ET, A new transgene reporter for in vivo magnetic resonance imaging, Nature Medicine 11(4) (2005) 450–454.

[25]. Grammatikopoulos P, Steinhauer S, Vernieres J, Singh V, Sowwan M, Nanoparticle design by gas-phase synthesis, Advances in Physics: X 1(1) (2016) 81–100.

[26]. Zurkiya O, Chan AW, Hu X, MagA is sufficient for producing magnetic nanoparticles in mammalian cells, making it an MRI reporter, Magn Reson Med 59(6) (2008) 1225–31. [PubMed: 18506784]

[27]. Mascolo M, Pei Y, Ring T, Room Temperature Co-Precipitation Synthesis of Magnetite Nanoparticles in a Large pH Window with Different Bases, Materials 6(12) (2013) 5549–5567. [PubMed: 28788408]

[28]. Reynolds F, O'Loughlin T, Weissleder R, Josephson L, Method of Determining Nanoparticle Core Weight, Analytical Chemistry 77(3) (2005) 814–817. [PubMed: 15679348]

[29]. Sun S, Zeng H, Robinson DB, Raoux S, Rice PM, Wang SX, Li G, Monodisperse MFe2O4(M = Fe, Co, Mn) Nanoparticles, Journal of the American Chemical Society 126(1) (2004) 273–279. [PubMed: 14709092]

[30]. Park J, An K, Hwang Y, Park J-G, Noh H-J, Kim J-Y, Park J-H, Hwang N-M, Hyeon T, Ultra-large-scale syntheses of monodisperse nanocrystals, Nature Materials 3(12) (2004) 891–895. [PubMed: 15568032]

[31]. Xie J, Xu C, Kohler N, Hou Y, Sun S, Controlled PEGylation of Monodisperse Fe3O4 Nanoparticles for Reduced Non-Specific Uptake by Macrophage Cells, Advanced Materials 19(20) (2007) 3163–3166.

[32]. Lattuada M, Hatton TA, Functionalization of Monodisperse Magnetic Nanoparticles, Langmuir 23(4) (2007) 2158–2168. [PubMed: 17279708]

[33]. Qu H, Caruntu D, Liu H, O'Connor CJ, Water-Dispersible Iron Oxide Magnetic Nanoparticles with Versatile Surface Functionalities, Langmuir 27(6) (2011) 2271–2278. [PubMed: 21284390]

[34]. Tong S, Hou S, Ren B, Zheng Z, Bao G, Self-Assembly of Phospholipid–PEG Coating on Nanoparticles through Dual Solvent Exchange, Nano Letters 11(9) (2011) 3720–3726. [PubMed: 21793503]

[35]. Kim J, Kim HS, Lee N, Kim T, Kim H, Yu T, Song IC, Moon WK, Hyeon T, Multifunctional Uniform Nanoparticles Composed of a Magnetite Nanocrystal Core and a Mesoporous Silica Shell for Magnetic Resonance and Fluorescence Imaging and for Drug Delivery, Angewandte Chemie International Edition 47(44) (2008) 8438–8441. [PubMed: 18726979]

[36]. Kim Y, Lee Chung B, Ma M, Mulder WJM, Fayad ZA, Farokhzad OC, Langer R, Mass Production and Size Control of Lipid–Polymer Hybrid Nanoparticles through Controlled Microvortices, Nano Letters 12(7) (2012) 3587–3591. [PubMed: 22716029]

[37]. Xie J, Chen K, Huang J, Lee S, Wang J, Gao J, Li X, Chen X, PET/NIRF/MRI triple functional iron oxide nanoparticles, Biomaterials 31(11) (2010) 3016–3022. [PubMed: 20092887]

[38]. Yang Z, Duan J, Wang J, Liu Q, Shang R, Yang X, Lu P, Xia C, Wang L, Dou K, Superparamagnetic iron oxide nanoparticles modified with polyethylenimine and galactose for siRNA targeted delivery in hepatocellular carcinoma therapy, International Journal of Nanomedicine Volume 13 (2018) 1851–1865.

[39]. Maeng JH, Lee D-H, Jung KH, Bae Y-H, Park I-S, Jeong S, Jeon Y-S, Shim C-K, Kim W, Kim J, Lee J, Lee Y-M, Kim J-H, Kim W-H, Hong S-S, Multifunctional doxorubicin loaded superparamagnetic iron oxide nanoparticles for chemotherapy and magnetic resonance imaging in liver cancer, Biomaterials 31(18) (2010) 4995–5006. [PubMed: 20347138]

[40]. Ludwig JA, Weinstein JN, Biomarkers in Cancer Staging, Prognosis and Treatment Selection, Nature Reviews Cancer 5(11) (2005) 845–856. [PubMed: 16239904]

[41]. Goulart LR, Vieira CU, Freschi APP, Capparelli FE, Fujimura PT, Almeida JF, Ferreira LF, Goulart IMB, Brito-Madurro AG, Madurro JM, Biomarkers for Serum Diagnosis of Infectious Diseases and Their Potential Application in Novel Sensor Platforms, Critical Reviews™ in Immunology 30(2) (2010) 201–222.

[42]. Mazzara S, Sinisi A, Cardaci A, Rossi RL, Muratori L, Abrignani S, Bombaci M, Two of Them Do It Better: Novel Serum Biomarkers Improve Autoimmune Hepatitis Diagnosis, PLoS One 10(9) (2015) e0137927. [PubMed: 26375394]

[43]. Zhang L, Tong S, Zhou J, Bao G, Accurate Quantification of Disease Markers in Human Serum Using Iron Oxide Nanoparticle-linked Immunosorbent Assay, Theranostics 6(9) (2016) 1353–1361. [PubMed: 27375784]

[44]. Ahirwar R, Nahar P, Development of a label-free gold nanoparticle-based colorimetric aptasensor for detection of human estrogen receptor alpha, Anal Bioanal Chem 408(1) (2016) 327–32. [PubMed: 26476919]

[45]. Tong S, Ren B, Zheng Z, Shen H, Bao G, Tiny grains give huge gains: nanocrystal-based signal amplification for biomolecule detection, ACS Nano 7(6) (2013) 5142–50. [PubMed: 23659350]

[46]. Quinto CA, Mohindra P, Tong S, Bao G, Multifunctional superparamagnetic iron oxide nanoparticles for combined chemotherapy and hyperthermia cancer treatment, Nanoscale 7(29) (2015) 12728–12736. [PubMed: 26154916]

[47]. Tong S, Quinto CA, Zhang L, Mohindra P, Bao G, Size-Dependent Heating of Magnetic Iron Oxide Nanoparticles, ACS Nano 11(7) (2017) 6808–6816. [PubMed: 28625045]

[48]. Bauer LM, Situ SF, Griswold MA, Samia ACS, High-performance iron oxide nanoparticles for magnetic particle imaging – guided hyperthermia (hMPI), Nanoscale 8(24) (2016) 12162–12169. [PubMed: 27210742]

[49]. Sugumaran PJ, Liu XL, Herng TS, Peng E, Ding J, GO-Functionalized Large Magnetic Iron Oxide Nanoparticles with Enhanced Colloidal Stability and Hyperthermia Performance, ACS Appl Mater Interfaces 11(25) (2019) 22703–22713. [PubMed: 31244027] * This work demonstrates that PEGylated MIONs reside in the graphene oxide sheet have very high heating capacity under alternating magnetic field

[50]. Dadfar SM, Camozzi D, Darguzyte M, Roemhild K, Varvara P, Metselaar J, Banala S, Straub M, Guvener N, Engelmann U, Slabu I, Buhl M, van Leusen J, Kogerler P, Hermanns-Sachweh B, Schulz V, Kiessling F, Lammers T, Size-isolation of superparamagnetic iron oxide nanoparticles

improves MRI, MPI and hyperthermia performance, J Nanobiotechnology 18(1) (2020) 22. [PubMed: 31992302]

[51]. Carrey J, Mehdaoui B, Respaud M, Simple models for dynamic hysteresis loop calculations of magnetic single-domain nanoparticles: Application to magnetic hyperthermia optimization, Journal of Applied Physics 109(8) (2011) 083921.

[52]. Raikher YL, Stepanov VI, Perzynski R, Dynamic hysteresis of a superparamagnetic nanoparticle, Physica B: Condensed Matter 343(1–4) (2004) 262–266.

[53]. Rosensweig RE, Heating magnetic fluid with alternating magnetic field, Journal of Magnetism and Magnetic Materials 252 (2002) 370–374.

[54]. Lee J-H, Jang J-T, Choi J-S, Moon SH, Noh S-H, Kim J-W, Kim J-G, Kim I-S, Park KI, Cheon J, Exchange-coupled magnetic nanoparticles for efficient heat induction, Nature Nanotechnology 6(7) (2011) 418–422.

[55]. Chen R, Christiansen MG, Anikeeva P, Maximizing Hysteretic Losses in Magnetic Ferrite NanoparticlesviaModel-Driven Synthesis and Materials Optimization, ACS Nano 7(10) (2013) 8990–9000. [PubMed: 24016039]

[56]. Jones SK, Winter JG, Gray BN, Treatment of experimental rabbit liver tumours by selectively targeted hyperthermia, International Journal of Hyperthermia 18(2) (2002) 117–128. [PubMed: 11911482]

[57]. Casula MF, Conca E, Bakaimi I, Sathya A, Materia ME, Casu A, Falqui A, Sogne E, Pellegrino T, Kanaras AG, Manganese doped-iron oxide nanoparticle clusters and their potential as agents for magnetic resonance imaging and hyperthermia, Physical Chemistry Chemical Physics 18(25) (2016) 16848–16855. [PubMed: 27282828]

[58]. Sun C, Lee JSH, Zhang M, Magnetic nanoparticles in MR imaging and drug delivery, Advanced Drug Delivery Reviews 60(11) (2008) 1252–1265. [PubMed: 18558452]

[59]. Lee JI, Narayan M, Barrett JS, Analysis and comparison of active constituents in commercial standardized silymarin extracts by liquid chromatography–electrospray ionization mass spectrometry, Journal of Chromatography B 845(1) (2007) 95–103.

[60]. Tromsdorf UI, Bigall NC, Kaul MG, Bruns OT, Nikolic MS, Mollwitz B, Sperling RA, Reimer R, Hohenberg H, Parak WJ, Förster S, Beisiegel U, Adam G, Weller H, Size and Surface Effects on the MRI Relaxivity of Manganese Ferrite Nanoparticle Contrast Agents, Nano Letters 7(8) (2007) 2422–2427. [PubMed: 17658761]

[61]. Wei H, Bruns OT, Kaul MG, Hansen EC, Barch M, Wi niowska A, Chen O, Chen Y, Li N, Okada S, Cordero JM, Heine M, Farrar CT, Montana DM, Adam G, Ittrich H, Jasanoff A, Nielsen P, Bawendi MG, Exceedingly small iron oxide nanoparticles as positive MRI contrast agents, Proceedings of the National Academy of Sciences 114(9) (2017) 2325–2330.

[62]. Zhao Z, Zhou Z, Bao J, Wang Z, Hu J, Chi X, Ni K, Wang R, Chen X, Chen Z, Gao J, Octapod iron oxide nanoparticles as high-performance T2 contrast agents for magnetic resonance imaging, Nature Communications 4(1) (2013).

[63]. Nitin N, Laconte LEW, Zurkiya O, Hu X, Bao G, Functionalization and peptide-based delivery of magnetic nanoparticles as an intracellular MRI contrast agent, JBIC Journal of Biological Inorganic Chemistry 9(6) (2004) 706–712. [PubMed: 15232722]

[64]. Li F, Liang Z, Liu J, Sun J, Hu X, Zhao M, Liu J, Bai R, Kim D, Sun X, Hyeon T, Ling D, Dynamically Reversible Iron Oxide Nanoparticle Assemblies for Targeted Amplification of T1-Weighted Magnetic Resonance Imaging of Tumors, Nano Letters 19(7) (2019) 4213–4220. [PubMed: 30719918]

[65]. Shen C, Wang X, Zheng Z, Gao C, Chen X, Zhao S, Dai Z, Doxorubicin and indocyanine green loaded superparamagnetic iron oxide nanoparticles with PEGylated phospholipid coating for magnetic resonance with fluorescence imaging and chemotherapy of glioma, Int J Nanomedicine 14 (2019) 101–117. [PubMed: 30587988] * This paper describes the MIONs loaded with doxorubicin (DOX) and indocyanine green (ICG) could serve as a nanoprobe for MR and fluorescence imaging, and as a vehicle to deliver chemotherapeutic drugs for the treatment of glioma.

[66]. Shi D, Sadat ME, Dunn AW, Mast DB, Photo-fluorescent and magnetic properties of iron oxide nanoparticles for biomedical applications, Nanoscale 7(18) (2015) 8209–8232. [PubMed: 25899408]

[67]. Ederhy S, Mansencal N, Réant P, Piriou N, Barone-Rochette G, Role of multimodality imaging in the diagnosis and management of cardiomyopathies, Archives of Cardiovascular Diseases 112(10) (2019) 615–629. [PubMed: 31607558]

[68]. Ghafoor S, Burger IA, Vargas AH, Multimodality Imaging of Prostate Cancer, Journal of Nuclear Medicine 60(10) (2019) 1350–1358. [PubMed: 31481573]

[69]. Lee H, Yu MK, Park S, Moon S, Min JJ, Jeong YY, Kang H-W, Jon S, Thermally Cross-Linked Superparamagnetic Iron Oxide Nanoparticles: Synthesis and Application as a Dual Imaging Probe for Cancer in Vivo, Journal of the American Chemical Society 129(42) (2007) 12739–12745. [PubMed: 17892287]

[70]. Medarova Z, Pham W, Kim Y, Dai G, Moore A, In vivoimaging of tumor response to therapy using a dual-modality imaging strategy, International Journal of Cancer 118(11) (2006) 2796–2802. [PubMed: 16385568]

[71]. Kim D, Yu MK, Lee TS, Park JJ, Jeong YY, Jon S, Amphiphilic polymer-coated hybrid nanoparticles as CT/MRI dual contrast agents, Nanotechnology 22(15) (2011) 155101. [PubMed: 21389582]

[72]. Li J, Hu Y, Yang J, Wei P, Sun W, Shen M, Zhang G, Shi X, Hyaluronic acid-modified Fe3O4@Au core/shell nanostars for multimodal imaging and photothermal therapy of tumors, Biomaterials 38 (2015) 10–21. [PubMed: 25457979]

[73]. Chertok B, Moffat BA, David AE, Yu F, Bergemann C, Ross BD, Yang VC, Iron oxide nanoparticles as a drug delivery vehicle for MRI monitored magnetic targeting of brain tumors, Biomaterials 29(4) (2008) 487–496. [PubMed: 17964647]

[74]. Kayal S, Ramanujan RV, Doxorubicin loaded PVA coated iron oxide nanoparticles for targeted drug delivery, Materials Science and Engineering: C 30(3) (2010) 484–490.

[75]. Zhu X, Li J, Peng P, Hosseini Nassab N, Smith BR, Quantitative Drug Release Monitoring in Tumors of Living Subjects by Magnetic Particle Imaging Nanocomposite, Nano Lett 19(10) (2019) 6725–6733. [PubMed: 31498999] * This paper shows the use of iron oxide nanoclusters to deliver a chemotherapy drug in vivo and to track drug delivery via magnetic particle imaging (MPI).

[76]. Hadjipanayis CG, Machaidze R, Kaluzova M, Wang L, Schuette AJ, Chen H, Wu X, Mao H, EGFRvIII Antibody–Conjugated Iron Oxide Nanoparticles for Magnetic Resonance Imaging–Guided Convection-Enhanced Delivery and Targeted Therapy of Glioblastoma, Cancer Research 70(15) (2010) 6303–6312. [PubMed: 20647323]

[77]. Kohler N, Sun C, Wang J, Zhang M, Methotrexate-Modified Superparamagnetic Nanoparticles and Their Intracellular Uptake into Human Cancer Cells, Langmuir 21(19) (2005) 8858–8864. [PubMed: 16142971]

[78]. Zhang Y, Yang M, Park J-H, Singelyn J, Ma H, Sailor MJ, Ruoslahti E, Ozkan M, Ozkan C, A Surface-Charge Study on Cellular-Uptake Behavior of F3-Peptide-Conjugated Iron Oxide Nanoparticles, Small 5(17) (2009) 1990–1996. [PubMed: 19554564]

[79]. Hauser AK, Mitov MI, Daley EF, McGarry RC, Anderson KW, Hilt JZ, Targeted iron oxide nanoparticles for the enhancement of radiation therapy, Biomaterials 105 (2016) 127–135. [PubMed: 27521615]

[80]. Alexiou C, Arnold W, Klein RJ, Parak FG, Hulin P, Bergemann C, Erhardt W, Wagenpfeil S, Lübbe AS, Locoregional cancer treatment with magnetic drug targeting, Cancer Res 60(23) (2000) 6641–8. [PubMed: 11118047]
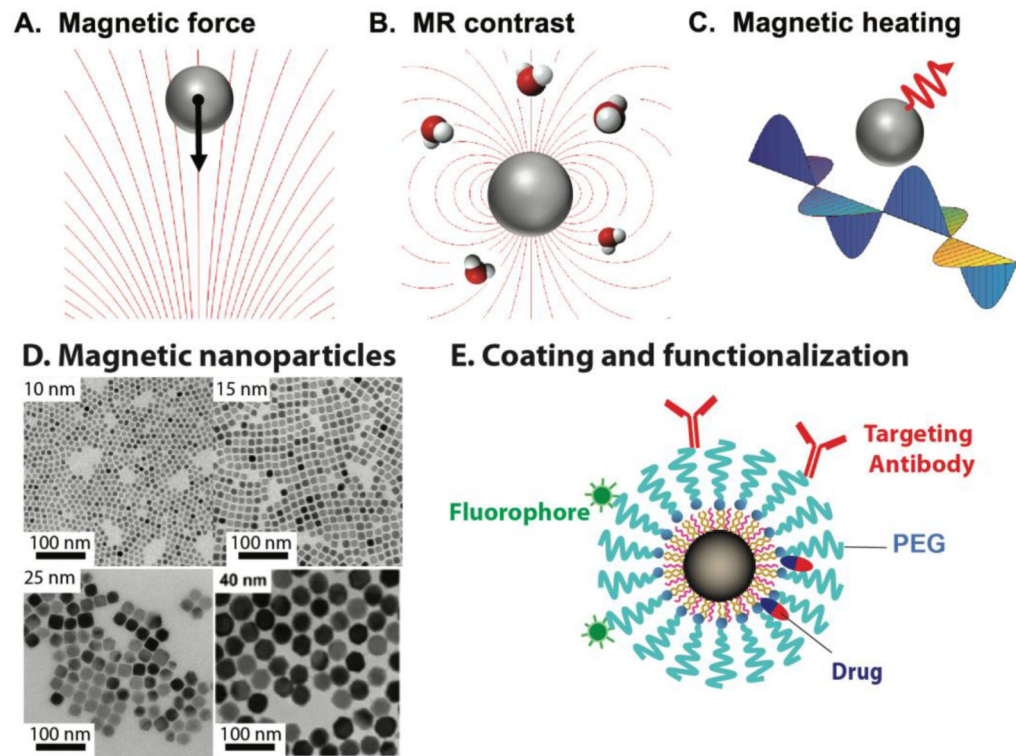
Figure 1. Magnetic iron oxide nanoparticles (MIONs) and their biomedical applications.
A, **B,** and **C** illustrate the three main magnetic properties of MIONs used in biomedical applications. **A**. Magnetic force generated by the interaction of MIONs with a nonuniform magnetic field. **B**. Magnetic resonance imaging (MRI) contrast due to the effect of MIONs on the relaxation of water protons. **C**. Magnetic heating generated by MIONs in an alternating magnetic field. **D**. TEM images of MIONs of 10, 15, 25 and 40 nm respectively. Scale bars equal 100 nm. **E**. A single MION coated with phospholipid-PEG and functionalized with targeting antibody, fluorescent dye, and drug molecules.
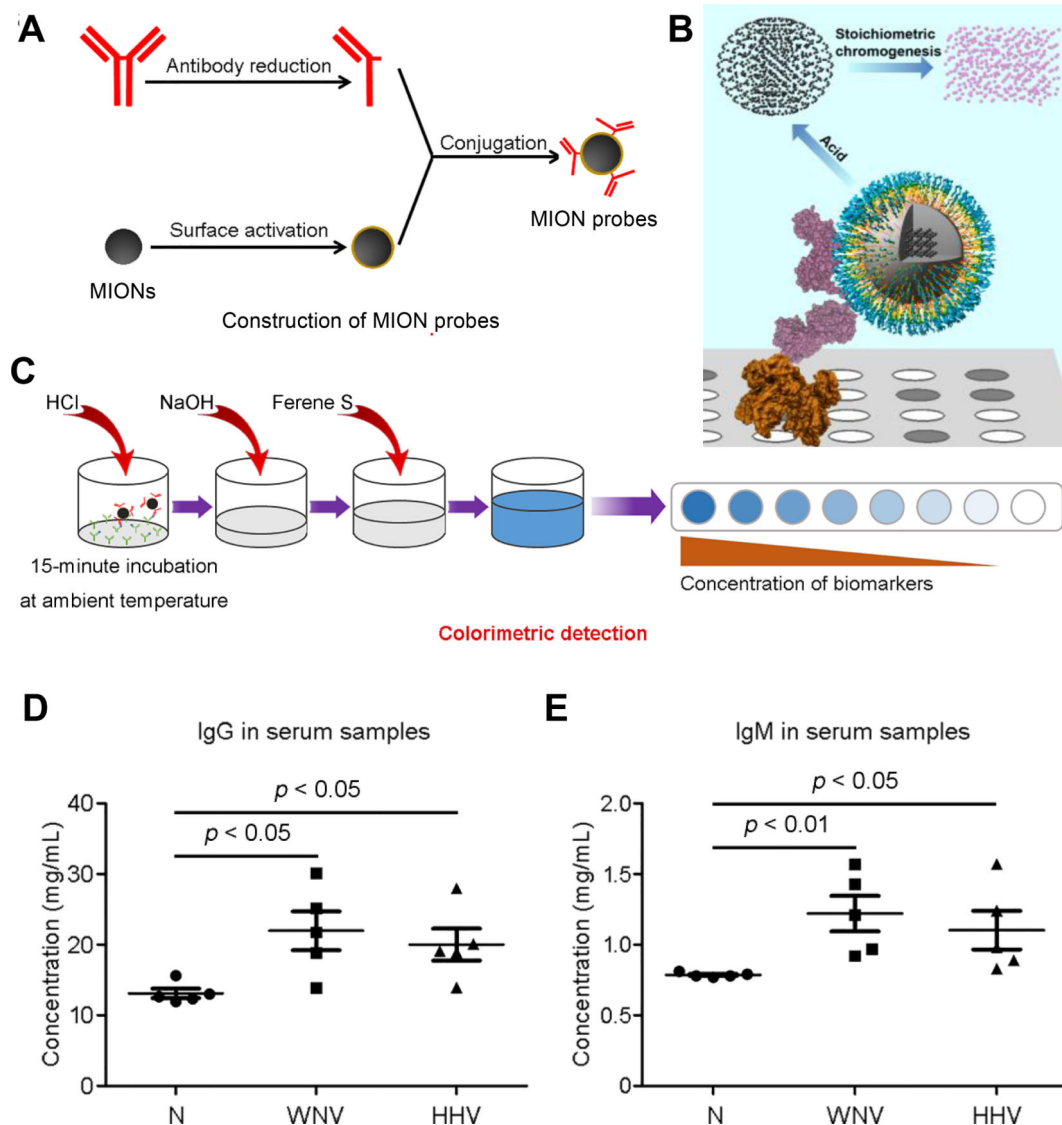
Figure 2. Iron oxide nanoparticle linked immunosorbent assay (ILISA).
A. Construction of detection probe in ILISA by conjugation of the detection antibody fragments to MION. **B**. A schematic showing an ILISA assay that quantifies proteins immobilized on a surface through binding of the MION probe. The MION probes bound to the target proteins are dissolved by acid into individual metal atoms which are converted to chromophores through a stoichiometric reaction **C**. The probes bound to the target molecules were measured using a colorimetric assay. Signal amplification is fully determined by the total number of atoms in the nanocrystals bound to a single target molecule. CDS, color development solution. **D** and **E**, The use of ILISA in quantifying IgG (D) and IgM (E) in serum samples of patients infected with West Nile virus (WNV) and human herpes virus (HHV) in comparison with healthy subjects (N).
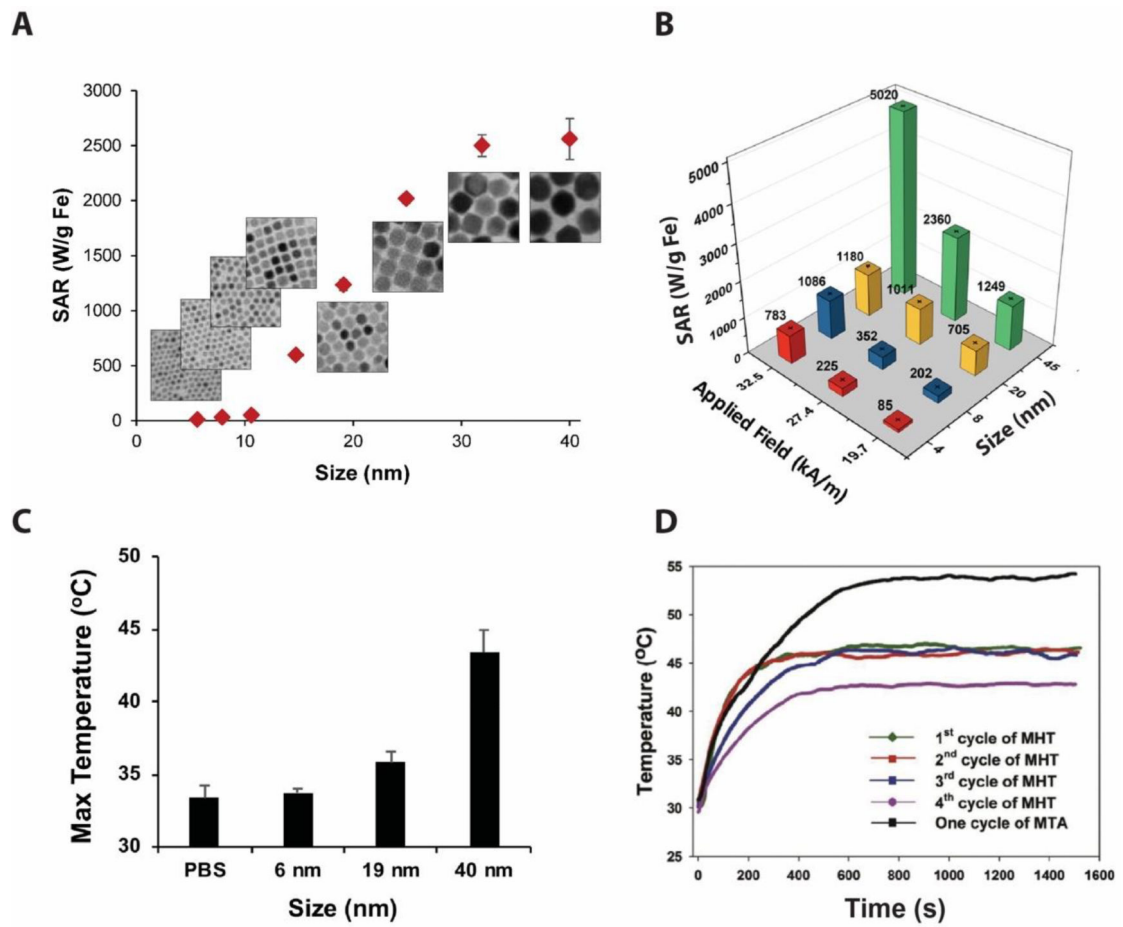
Figure 3. MIONs based magnetic heating and applications in hyperthermia treatment.
A. The heating capacity of MIONs increases with the size of iron oxide nanocrystals.
B. Size and field dependent heating of MIONs reside in a graphene oxide sheet. **C**. Temperature in U87 tumors in mice after injection of MIONs and applying alternating magnetic field for 1 h at 9.35 kA/m and 325 kHz. **D**. Elevated tumor temperature versus time induced by multiple magnetic hyperthermia therapy runs after a single injection of MIONs.
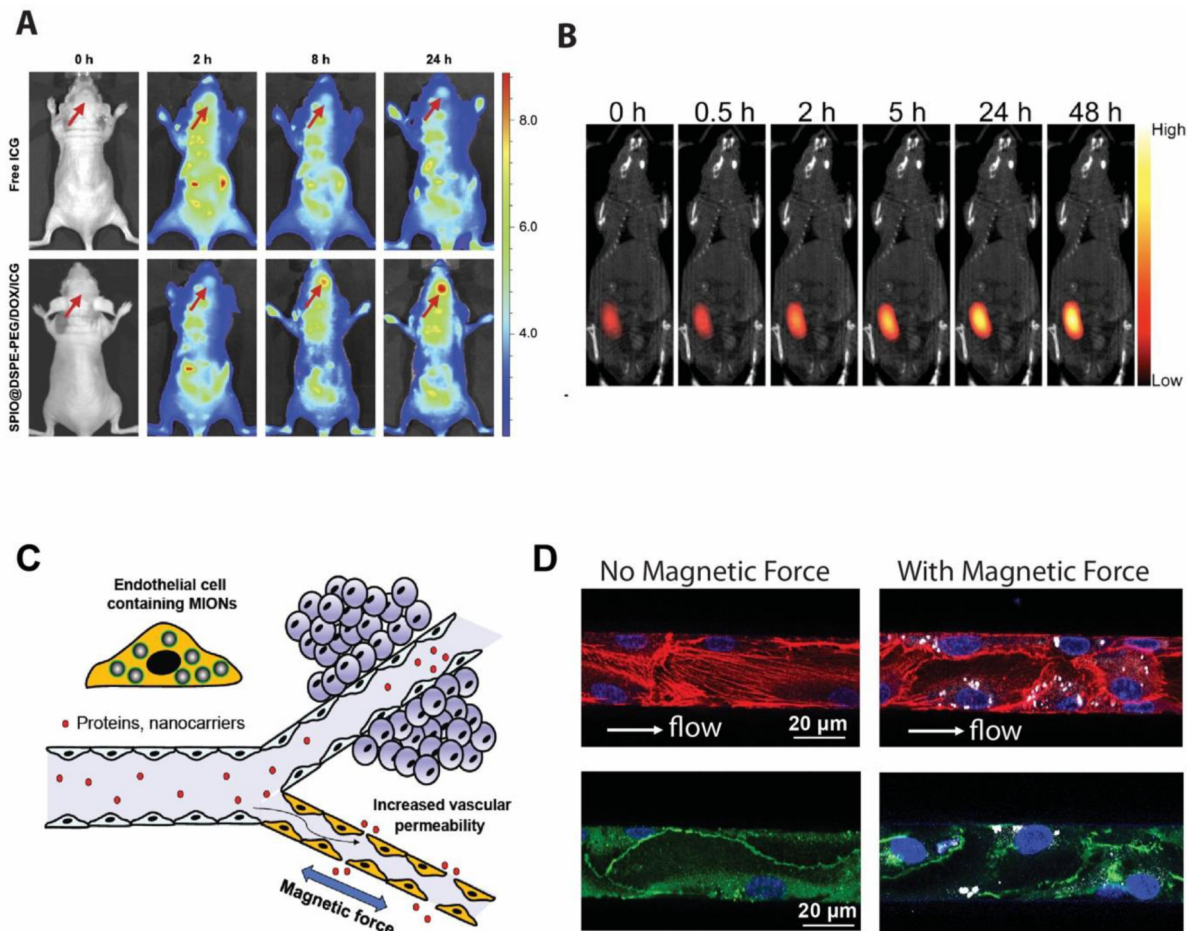
Figure 4. Application of MION for *in vivo* imaging and drug delivery.
A. Fluorescence images of glioma-bearing nude mice at different times after tail vein injection of free ICG and SPIO@DSPE-PEG/DOX/ICG NPs with arrows pointing at the location of glioma. **B**. Merged images of magnetic particle imaging (MPI, colored image) and X-ray computed tomography (CT, black and white) of an MDA-MB-231 tumor-bearing nude mouse injected intratumorally with iron oxide clusters containing Doxorubicin. **C**. A schematic illustration of the blood vessel that presents a major transport barrier to *in vivo* delivery by only allowing selective extravasation of solutes and small molecules, but not proteins and nanoparticles. When endothelial cells lining the interior surface of blood vessels have MIONs internalized, an applied magnetic field generates force in these cells, disrupting endothelial adherens junctions and increasing the vessel permeability, allowing proteins and nanocarriers to extravasate. **D**. MIONs are first delivered into endothelial cells in the microfluidic channels. After subjected to an applied magnetic field for 1 h after which the endothelialized channels were fixed and stained for actin and VE-cadherin. (Left) Without magnetic force, the endothelial actin filaments (red) were aligned along the flow direction and the adherens junctions were continuous (green). (Right) With applied magnetic forces, the number of actin filaments along the flow direction was reduced and the

distribution of VE-cadherin became discontinuous and diffuse, indicating the disruption of adherens junctions at intercellular interfaces.